Cell Reports Medicine, Volume *5*

Supplemental information

Targeted therapy improves cellular dysfunction, ataxia, and seizure susceptibility in a model of a progressive myoclonus epilepsy

Huijie Feng, Jerome Clatot, Keisuke Kaneko, Marco Flores-Mendez, Eric R. Wengert, Carly Koutcher, Emily Hoddeson, Emily Lopez, Demetrius Lee, Leroy Arias, Qiansheng Liang, Xiaohong Zhang, Ala Somarowthu, Manuel Covarrubias, Martin J. Gunthorpe, Charles H. Large, Naiara Akizu, and Ethan M. Goldberg

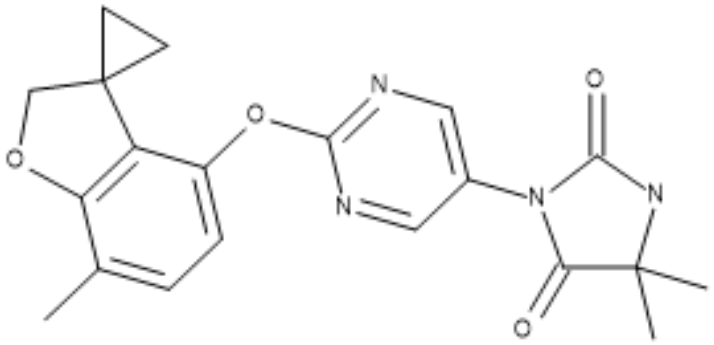

Figure S1. Chemical structure of AUT00206 (AUT6, or 5,5-dimethyl-3-[2-(7-methylspiro[2H-benzofuran-3,1'-cyclopropane]-4-yl)oxypyrimidin-5-yl]imidazolidine-2,4-dione). Related to STAR★ Methods.

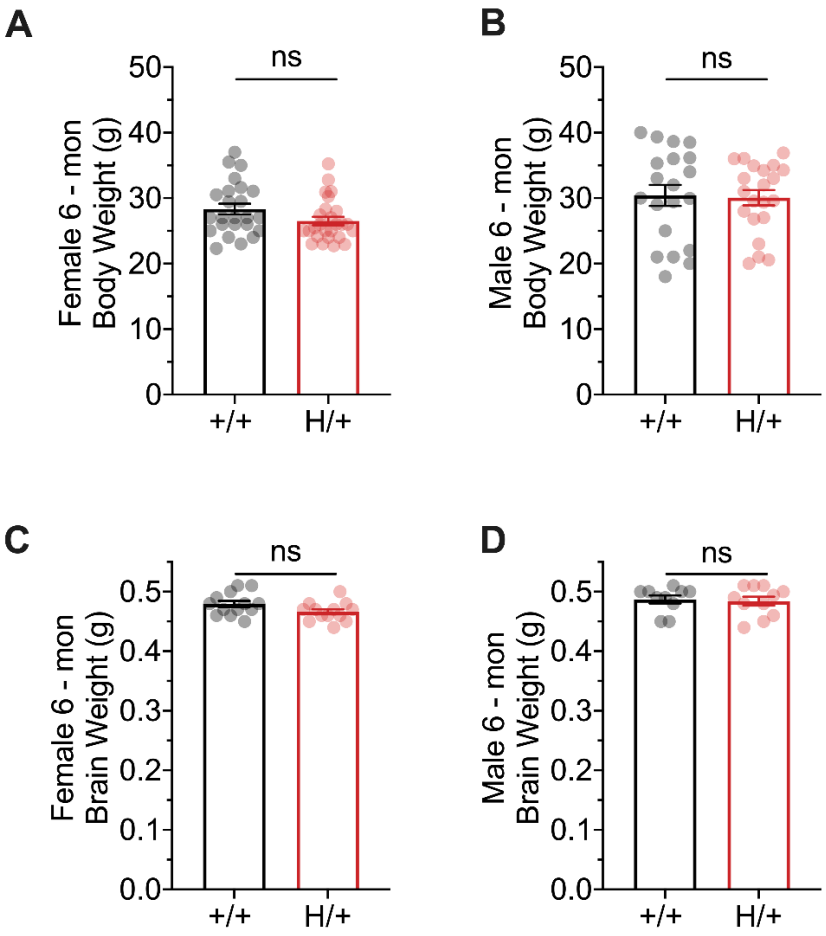

Figure S2. Body and brain weight show no genotype difference in either sex. Related to Figure 1.

(A-B) At 6 months of age, there is no difference in body weight between WT and H/+ mice for either females (A) or males (B).

(C-D) There is no difference in brain weight between WT and H/+ mice for either females (C) or males (D).

Data are presented as mean ± SEM. Statistical analyses: unpaired Student's t-test.

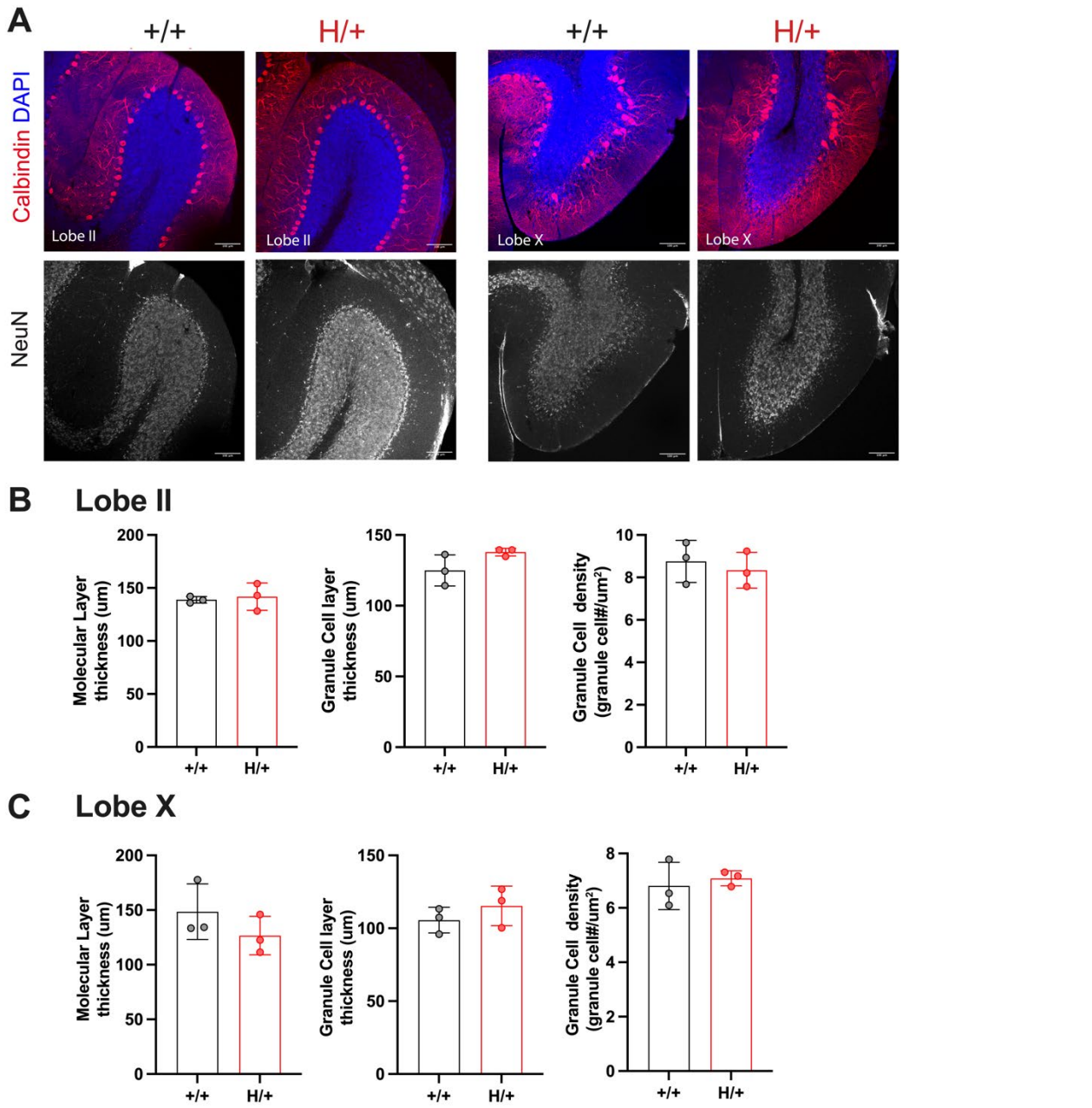

Figure S3. 9-month-old H/+ mice show no loss of cerebellar granule cells or Purkinje cells. Related to Figure 1.

(A) Examples of representative cerebellar lobes (Lobe II and Lobe X) for +/+ and H/+ mice at 9 months of age.

Quantification of cerebellar layer thickness of 9-month-old H/+ mice and WT littermate controls shows no significant difference in molecular layer sickness, granule cell layer thickness and granule cell density in Lobe II (B) and Lobe X (C).

Data are presented as mean ± SEM. Statistical analyses: unpaired Student's t-test.

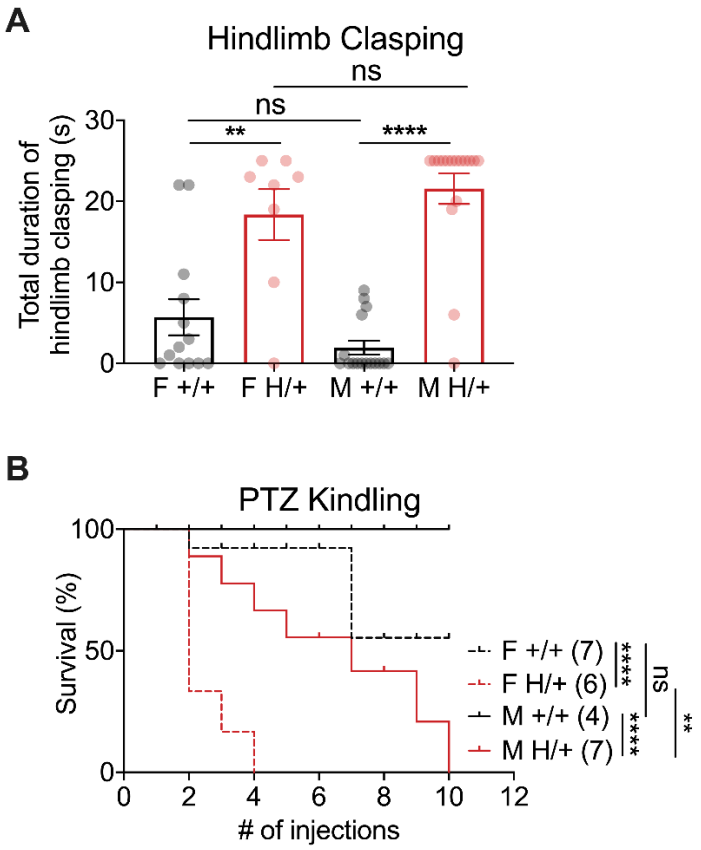

Figure S4. The main disease-related phenotypes identified in H/+ mice are present in both males and females. Related to Figure 3.

(A) Hindlimb clasping is an indicator of cerebellar dysfunction; genotype differences between H/+ and WT mice persist in a subgroup analysis of males and females only. There is no genotype difference in the performance of either male or female mice.

(B) Accelerated PTZ kindling epileptogenesis – a measure of cerebral cortex hyperexcitability and propensity to seizure – is present in both male and female H/+ mice relative to WT. Female H/+ mice are more prone to PTZ-induced kindling epileptogenesis than male H/+ mice.

Data are presented as mean ± SEM. Statistical analyses: (A) one-way ANOVA with Šídák's multiple comparison test; (B) Mantel-Cox Test;**, $p < 0.01$; ****, $p < 0.0001$.

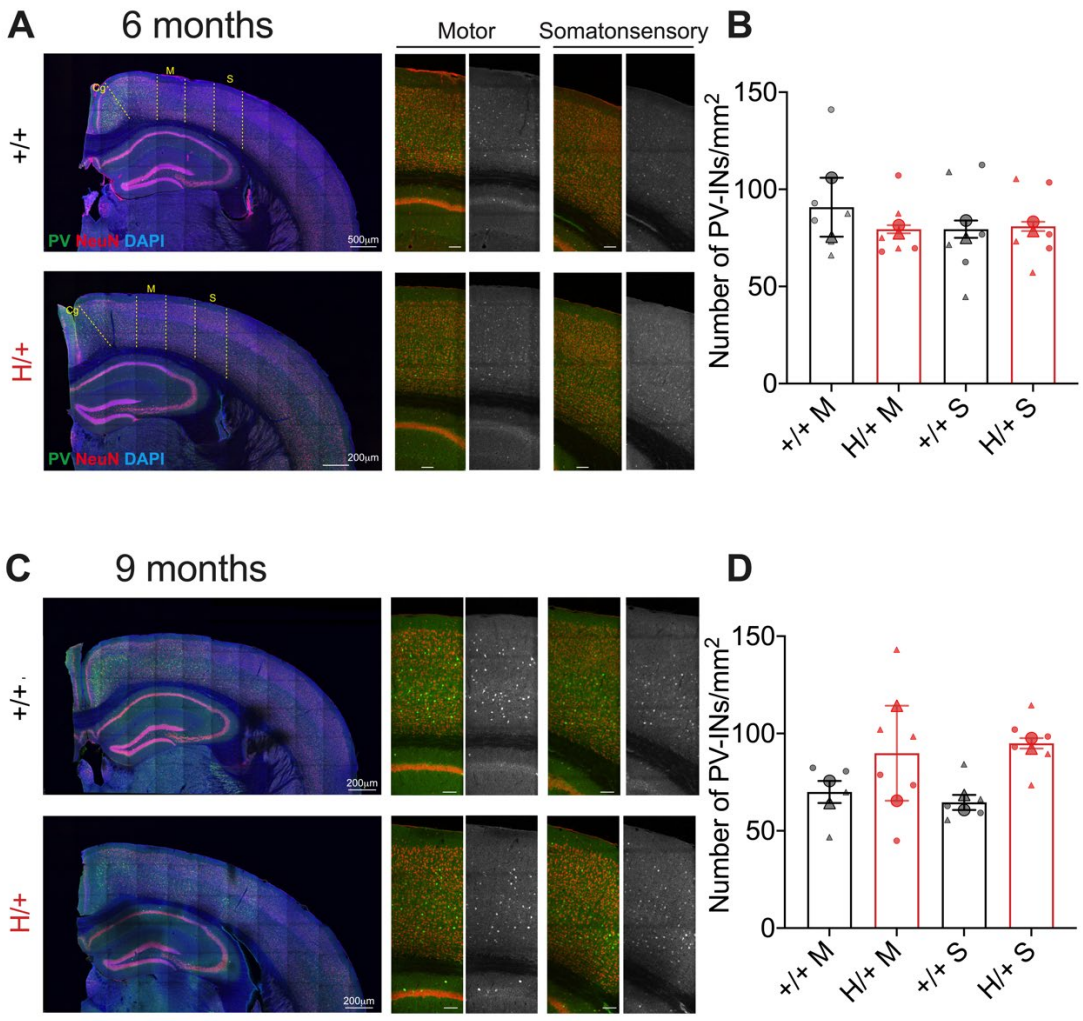

Figure S5. Normal neocortical GABAergic PV-IN numbers in H/+ mice. Related to Figure 1.

(A, C) The number of PV-INs is normal in H/+ mice. Shown is a representative image of motor and somatosensory neocortex demonstrating immunostaining with anti-pavalbumin and anti-NeuN antibodies and counterstaining with DAPI in coronal sections of 6- (A) or 9-month-old (C) +/+ and H/+ mice.

(B, D) Bar graphs show summary data, presented as mean (*large dots*) ± SEM of PV-IN density in $n = 2$ mice of each genotype (calculated from the average of 3 sections per mouse; *small dots*).

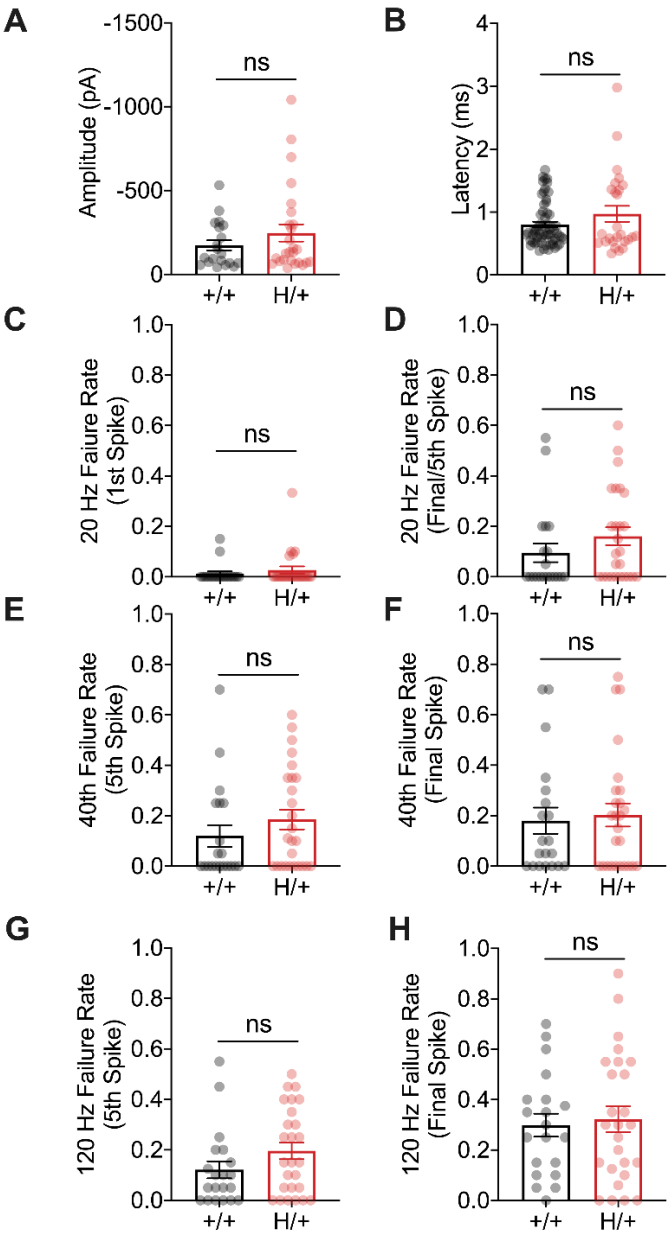

Figure S6. Features of unitary synaptic transmission at PV-IN:principal cell synapses in H/+ versus WT mice at P16-21. Related to Figure 5.

There is no significant difference in average unitary inhibitory postsynaptic current (uIPSC) amplitude (A) or latency (B) between +/+ and H/+ mice at P16-21. (C-H) Failure rate with 20, 40 or 120 Hz stimulation also shows no significant difference between +/+ and H/+ mice. Data are presented as mean ± SEM. Statistical analyses: unpaired Student's t-test.

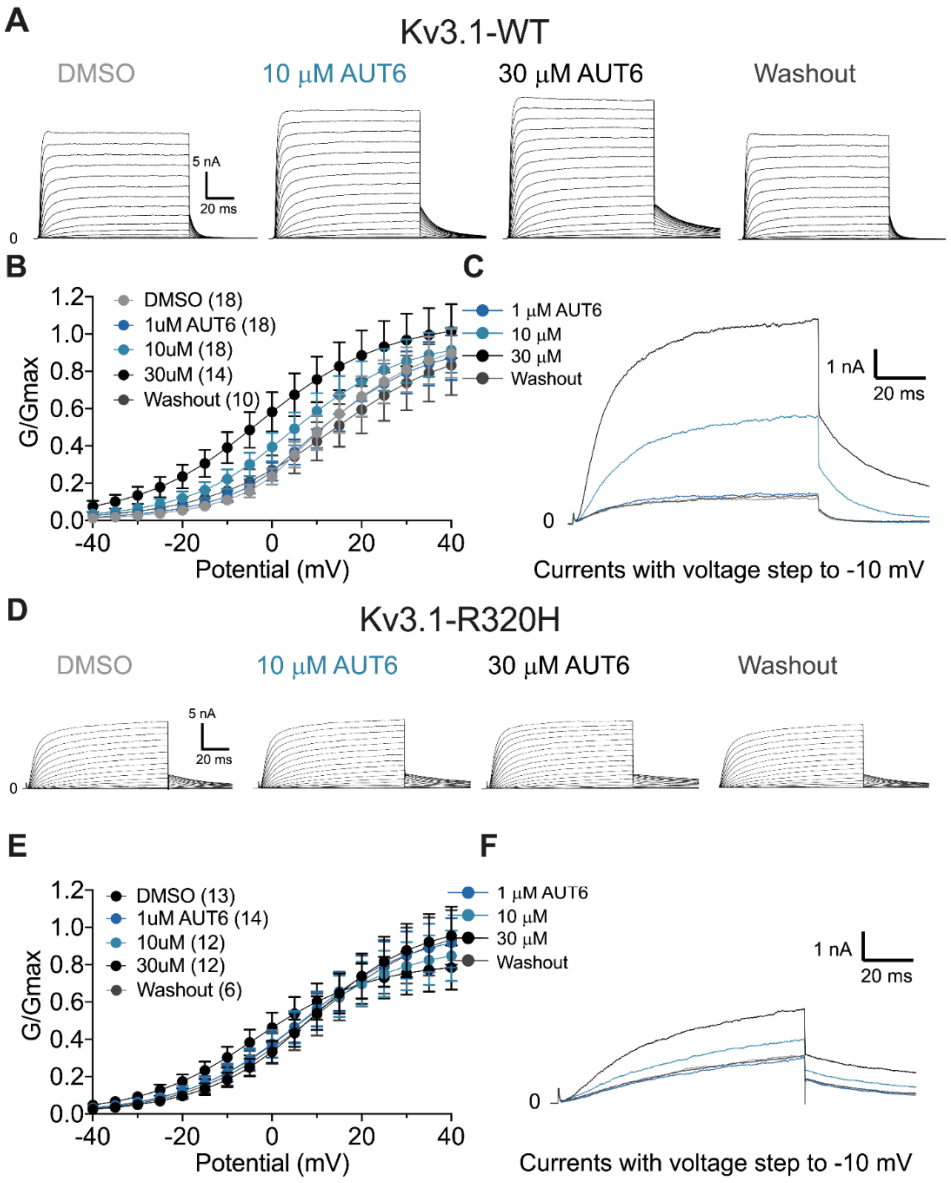

Figure S7. Biophysical properties of Kv3.1-WT and Kv3.1-Arg320His with activation by AUT00206. Related to Figure 6.

(A-C) Data for Kv3.1-WT. Shown are representative currents of HET-293T transiently transfected with Kv3.1-WT alone in response to increasing concentrations of AUT00206 along with washout (A), and corresponding with G/Gmax curves (B). (C) Overlay of currents in response to a voltage step to -10 mV to highlight the effect of AUT00206.

(D-F) as in (A-C), but for HET-293T cells transiently transfected with the Kv3.1-Arg320His variant alone. Note lower peak and steady-state currents relative to Kv3.1-WT but with clear activation by AUT00206 in the raw traces (D) and G/Gmax curves (E). The effect of AUT00206 on Kv3.1-Arg320His is highlighted via overlay of the response to voltage steps to -10 mV (F).

Data are presented as Mean ± SEM.

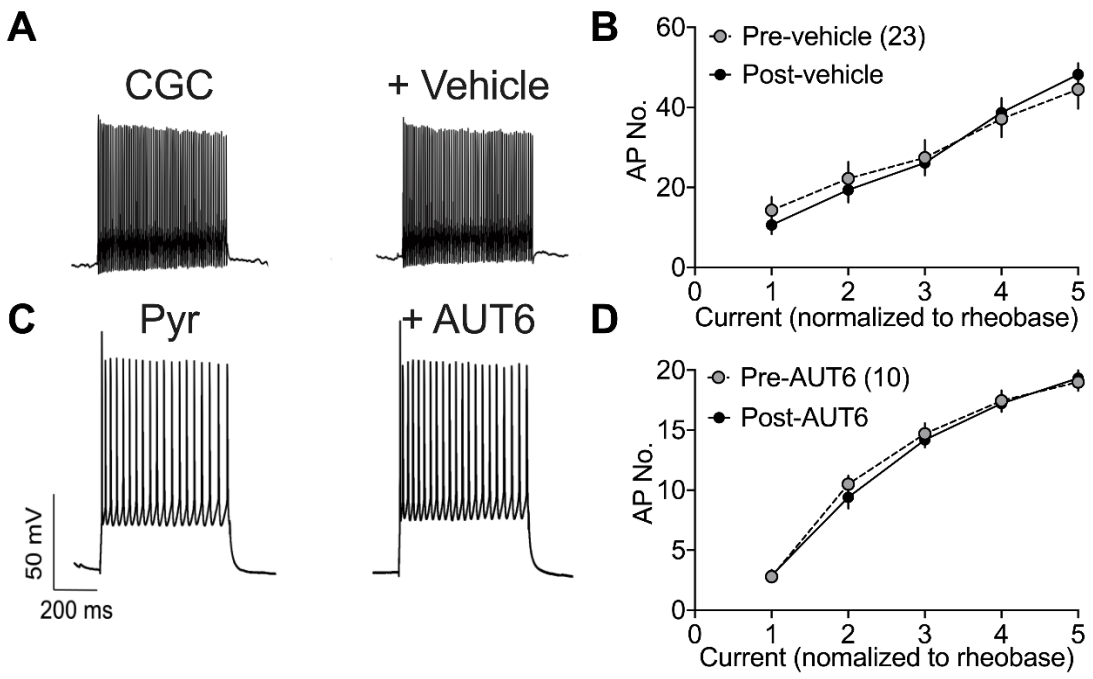

Figure S8. Specificity of AUT00206 for Kv3-expressing neurons. Related to Figure 6.

(A-B) Vehicle has no effect on the electrical excitability of cerebellar granule cells.

(C-D) AUT00206 has no effect on neocortical pyramidal neurons, which do not express Kv3 channels.

Data are presented as Mean ± SEM. Statistical analyses: Two-way ANOVA with Šídák's multiple comparison test.

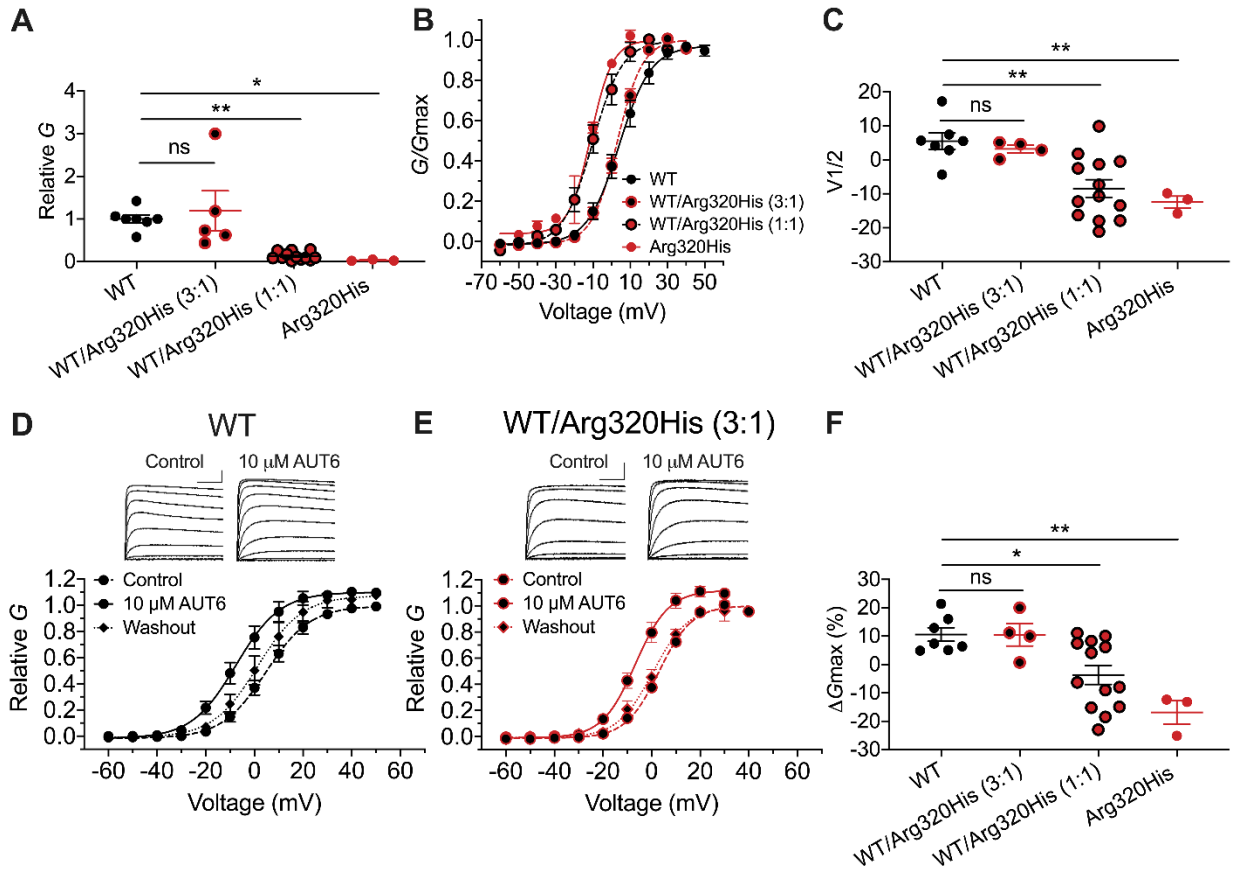

Figure S9. Properties of human *KCNC1*-p. Arg320His and effect of AUT00206 in *Xenopus* oocytes. Related to Figure 6.

Shown are results of two-electrode voltage-clamp recordings of wild-type and variant *KCNC1* expressed in *Xenopus* oocytes.

(A) Plot of relative conductance (*G/Gmax*; y-axis) for wild-type Kv3.1 (WT; *black circles*), Kv3.1- Arg320His (Arg320His; *red circles*), and 3:1 (*black circles with red borders*) or 1:1 mixtures of WT and Arg320His RNA (*red circles with black borders*). Note that Arg320His alone produces essentially no current, while mixtures of WT and Arg320His produce intermediate levels of current consistent with a dominant negative effect of the Arg320His -containing subunit. Note that identical amounts of RNA were injected in all experimental conditions at a concentration of 36 ng/uL.

(B) *G-V* plots showing a left shift in the voltage dependence of activation for Arg320His alone and with a 1:1 mixture with WT (but not at 3:1 mixture), and increased conductance at/around 0 mV for Arg320His and 1:1.

(C) Quantification of (B) with plot of voltage at half-maximal activation ($V_{1/2}$) for each group.

(D-F) AUT00206 produces increased conductance of WT Kv3.1 (D) and WT/Arg320His at a 3:1 ratio (E), but not with a 1:1 ratio. R320H alone produces very small currents (*not shown*). (F) quantification of relative changes in *G*max from the data in D and E. (D-E*)*.
Data are presented as Mean ± SEM. Statistical analyses: One-way ANOVA with Šídák's multiple comparison test, * $p< 0.05$; ** $p < 0.01$.

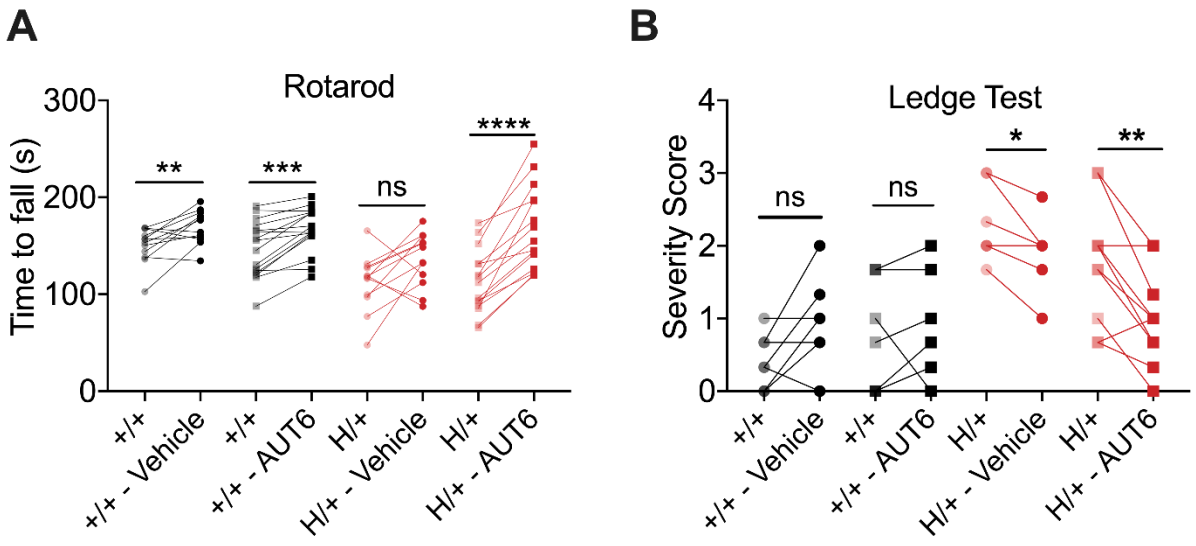

Figure S10. Effect of a single i.p. dose of AUT00206 (30 mg/kg) on the performance of WT and H/+ mice on the Rotarod and Ledge Test. Related to Figure 6.

While we did observe a learning effect in the motor behavioral tests, a single i.p. injection of 30 mg/kg AUT6 still significantly improved the performance of 6-month-old mice on the Rotarod (A) and in the Ledge Test (B).

Data are presented as mean ± SEM. Statistical analysis via paired t-test. * $p < 0.05$, ** $p < 0.01$, *** $p < 0.001$, **** $p < 0.0001$.

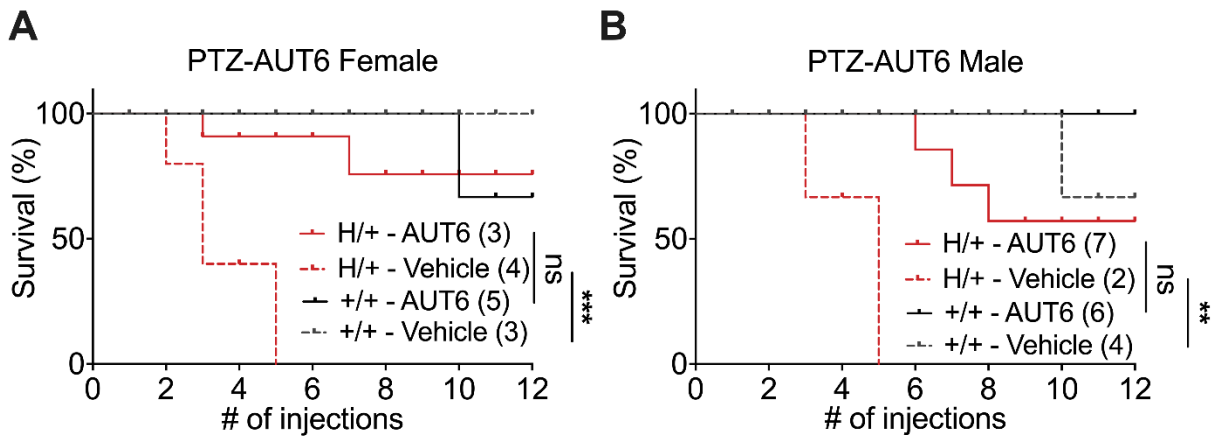

Figure S11. The effect of AUT00206 on kindling epileptogenesis in H/+ mice persists in both male and female mice. Related to Figure 6.

Treatment of AUT00206 eliminates the difference between H/+ and +/+ groups in both female (A) and male (B) mice.

Mantel-Cox Test;**, $p < 0.01$; ***, $p < 0.001$.

Table S1 appears in a separate Excel file.

				Intrinsic Membrane Properties				
Genotype	Age	Mice (*N*)	Cells (*n*)	V_m	R_m	Tau	Sag	Rheobase
				mV	MOhms	ms	%	pA
H/H	P16-21	3	19	-69.8 ± 2.4	1820 ± 258	12.8 ± 1.5	6 ± 1**	19.6 ± 3.1
H/+	P16-21	4	39	-78.6 ± 2.3	2376 ± 219	16.2 ± 1.7	12 ± 2*	16.3 ± 2.2
	2-mo	3	23	-81.0 ± 1.5	1314 ± 150	9.82 ± 1.06	11 ± 2	25.6 ± 3.5
	4-mo	2	20	-80.9 ± 1.9	1109 ± 151	8.72 ± 0.81	14 ± 2	40.6 ± 5.1*
	6-mo	13	50	-75.1 ± 1.6	2068 ± 173	13.9 ± 1.1	12 ± 1	19.4 ± 2.2
+/+	P16-21	4	39	-72.1 ± 2.0	1676 ± 222	12.7 ±1.4	22 ± 4	15.5 ± 1.5
	2-mo	3	23	-81.4 ± 1.9	1267 ± 113	10.6 ± 1.2	13 ± 2	29.5 ± 2.8
	4-mo	2	20	-79.3 ± 1.3	1189 ± 137	9.40 ± 1.46	12 ± 1	25.1 ± 2.9
	6-mo	13	40	-78.1 ± 1.9	2593 ± 286	15.1 ± 1.5	9 ± 1	17.1 ± 2.9
p values (via via One-way ANOVA or unpaired Student's t-test, vs. age-matched +/+ mice)								
P16-21	H/H vs. +/+			0.809	0.898	0.999	0.002	0.417
P16-21	H/+ vs. +/+			0.106	0.052	0.237	0.016	0.952
2-mo	H/+ vs. +/+			0.878	0.802	0.641	0.565	0.377
4-mo	H/+ vs. +/+			0.474	0.697	0.679	0.419	0.042
6-mo	H/+ vs. +/+			0.230	0.105	0.535	0.204	0.536

Table S2. Intrinsic membrane properties of cerebellar granule cells by genotype and age. Related to Figure 4.

*, $p < 0.05$; **, $p < 0.01$; ***, $p < 0.001$

				Action Potential Properties										
Group	Age	Mice (*N*)	Cells (*n*)	Inflection Rate	Max Rise Slope	AP Thres-hold	AP Amp-litude	AP Peak	AP Rise Time	AP Halfwidth	AHP Amp-litude	AHP Time	ISI CoV
				mV/ms	mV/ms	mV	mV	mV	ms	ms	mV	ms	
H/H	P16-21	3	19	12.9 ± 2.6*	435 ± 44*	-45.2 ±1.2	71.5 ± 3.1*	26.3 ± 3.0	0.62 ± 0.06	0.44 ± 0.02***	-21.4 ± 0.8*	2.0 ± 0.36***	0.39 ± 0.06**
H/+	P16-21	4	39	18.5 ± 2.6	346 ± 20	-42.9 ± 0.6	66.3 ± 1.8	23.4 ± 1.9	0.57 ± 0.02	0.40 ± 0.01*	-23.3 ± 0.6	1.42 ± 0.08	0.26 ± 0.03**
	2-mo	3	23	20.5 ± 4.1	392 ± 18***	-45.7 ± 0.9	67.5 ± 1.4***	21.8 ± 1.5***	0.63 ± 0.05	0.34 ± 0.01**	-25.1 ± 0.5	1.24 ± 0.05***	0.22 ± 0.03*
	4-mo	2	22	20.9 ± 4.6	337 ± 18**	-42.0 ± 1.1	64.3 ± 1.7***	22.3 ± 1.7***	0.62 ± 0.05	0.38 ± 0.01*	-26.4 ± 1.0	1.31 ± 0.06**	0.29 ± 0.05
	6-mo	13	50	18.9 ± 2.4	296 ± 15*	-42.2 ± 0.7	61.7 ± 1.7*	19.5 ± 1.5*	0.62 ± 0.03	0.40 ± 0.01*	-25.9 ± 0.5	1.48 ± 0.06***	0.26 ± 0.03
+/+	P16-21	4	39	28.7 ± 5.3	333 ± 20	-42.4 ±1.1	63.7 ± 1.9	21.2 ± 1.9	0.53 ± 0.04	0.34 ± 0.02	-24.3 ± 0.7	1.01 ± 0.04	0.21 ± 0.02
	2-mo	3	23	24.6 ± 3.4	285 ± 10	-44.2 ± 0.8	54.4 ± 1.4	10.2 ± 1.4	0.57 ± 0.03	0.31 ± 0.01	-26.5 ± 0.7	1.01 ± 0.04	0.16 ± 0.02
	4-mo	2	22	18.6 ± 3.8	271 ± 15	-43.1 ± 1.3	54.7 ± 1.7	11.6 ± 2.0	0.51 ± 0.03	0.34 ± 0.01	-25.8 ± 0.8	1.08 ± 0.03	0.17 ± 0.03
	6-mo	13	50	21.3 ± 3.1	249 ± 9	-42.9 ± 1.0	57.4 ± 1.2	14.5 ± 1.2	0.62 ± 0.03	0.36 ± 0.01	-24.8 ± 0.6	1.20 ± 0.04	0.24 ± 0.03
p values (via via One-way ANOVA or unpaired Student's t-test, vs. age-matched +/+ mice)													
P16-21	H/H vs. +/+			0.017	0.028	0.112	0.044	0.236	0.240	0.001	0.024	<0.0001	0.002
P16-21	H/+ vs. +/+			0.075	0.902	0.900	0.556	0.668	0.718	0.020	0.477	0.002	0.497
2-mo	H/+ vs. +/+			0.440	<0.0001	0.236	<0.0001	<0.0001	0.309	0.004	0.157	0.0004	0.035
4-mo	H/+ vs. +/+			0.706	0.007	0.498	0.0003	0.0002	0.060	0.017	0.655	0.0020	0.052
6-mo	H/+ vs. +/+			0.522	0.015	0.558	0.049	0.015	0.977	0.015	0.192	0.0007	0.550

Table S3. Action potential properties of cerebellar granule cells by genotype and age. Related to Figure 4.

*, $p < 0.05$; **, $p < 0.01$; ***, $p < 0.001$

				Firing Frequency	
Genotype	Age	Mice (*N*)	Cells (*n*)	Steady-state	Instantaneous
				Hz	Hz
H/H	P16-21	3	19	95 ± 9****	141 ± 8****
H/+	P16-21	4	39	149 ± 6*	175 ± 6
	2-mo	3	23	134 ± 11***	174 ± 9***
	4-mo	2	22	100 ± 9***	148 ± 6***
	6-mo	13	50	101 ± 6***	138 ± 5***
+/+	P16-21	4	39	171 ± 7	199 ±7
	2-mo	3	23	187 ± 8	228 ± 8
	4-mo	2	22	172 ± 10	213 ± 7
	6-mo	13	50	161 ± 7	195 ± 7
p values (via via One-way ANOVA or unpaired Student's t-test, vs. age-matched +/+ mice)					
P16-21	H/H vs. +/+			<0.0001	<0.0001
P16-21	H/+ vs. +/+			0.0406	0.058
2-mo	H/+ vs. +/+			0.0002	<0.0001
4-mo	H/+ vs. +/+			<0.0001	<0.0001
6-mo	H/+ vs. +/+			<0.0001	<0.0001

Table S4. Firing frequency of cerebellar granule cells by genotype and age. Related to Figure 4.

*, $p < 0.05$; **, $p < 0.01$; ***, $p < 0.001$

					Intrinsic Membrane Properties				
Genotype	Age	Mice (*N*)	Cells (*n*)	V_m	R_m	Tau	Capacitance	Sag	Rheobase
				mV	MOhms	ms	pF	%	pA
H/H	P16-21	3	11	-71.2 ± 1.0	103 ± 8	7.7 ± 0.5	76.7 ± 5.1	6.2 ± 2.9	200 ± 36
H/+	P16-21	5	22	-71.4 ± 1.2**	99.3 ± 7.6	7.7 ± 0.9	86.5 ± 14.1	11.2 ± 1.5	200 ± 21
	6-mo	3	29	-64.3 ± 1.3**	149 ± 11*	10.3 ± 1.0**	76.6 ± 8.7	14.3 ± 2.4	169 ± 21
+/+	P16-21	3	13	-76.5 ± 1.1	112 ± 8	5.3 ± 0.6	68.6 ± 6.3	7.8 ± 0.7	177 ± 24
	6-mo	3	25	-70.0 ± 1.7	112 ± 9	5.9 ± 0.4	57.9 ± 4.9	9.2 ± 1.1	180 ± 15
	p values (via via One-way ANOVA or unpaired Student's t-test, vs. age-matched +/+ mice)								
P16-21	H/H vs. +/+			0.0178	0.7017	0.2494	0.8839	0.7931	0.7986
P16-21	H/+ vs. +/+			0.0067	0.4076	0.0641	0.4668	0.2846	0.7373
6-mo	H/+ vs. +/+			0.009	0.014	0.0003	0.0786	0.0655	0.6966

Table S5. Intrinsic membrane properties of neocortex PV+ GABAergic interneurons by genotype and age. Related to Figure 5.

*, $p < 0.05$; **, $p < 0.01$; ***, $p < 0.001$

				Action Potential Properties							
Group	Age	Mice (*N*)	Cells (*n*)	Max Rise Slope	AP Thres-hold	AP Amp-litude	AP Peak	AP Rise Time	AP Halfwidth	AHP Amp-litude	AHP Time
				mV/ms	mV	mV	mV	ms	ms	mV	ms
H/H	P16-21	3	11	421 ± 69	-45.1 ± 1.2	66.2 ± 5.1	21.1 ± 4.1	0.355 ± 0.033	0.40 ± 0.04**	-26.4 ± 1.0	1.9 ± 0.2***
H/+	P16-21	5	22	393 ± 30	-45.2 ± 0.9	62.0 ± 1.8	16.9 ± 1.9	0.317 ± 0.020	0.31 ± 0.02	-28.7 ± 1.0	1.3 ± 0.1
	6-mo	3	29	550 ± 54**	-42.1 ± 1.1	77.6 ± 2.4***	35.4 ± 3.0***	0.376 ± 0.033	0.39 ± 0.04*	-26.7 ± 1.3***	2.0 ± 0.1***
+/+	P16-21	3	13	439 ± 36	-47.9 ± 0.4	68.0 ± 2.7	20.1 ± 2.5	0.302 ± 0.015	0.30 ± 0.01	-27.9 ± 1.3	1.2 ± 0.1
	6-mo	3	25	360 ± 33	-42.1 ± 1.6	62.0 ± 2.3	19.9 ± 2.4	0.349 ± 0.014	0.29 ± 0.01	-26.2 ± 0.9	1.0 ± 0.04
p values (via via One-way ANOVA or unpaired Student's t-test, vs. age-matched +/+ mice)											
P16-21	H/H vs. +/+			0.9494	0.1672	0.8927	0.9639	0.2487	0.0079	0.6153	0.0004
P16-21	H/+ vs. +/+			0.6406	0.0933	0.2289	0.5571	0.8492	0.8775	0.8304	0.996
6-mo	H/+ vs. +/+			0.006	0.9919	<0.0001	0.0002	0.4809	0.025	<0.0001	<0.0001

Table S6. Action potential properties of neocortex PV+ GABAergic interneurons by genotype and age.
Related to Figure 5.

*, $p < 0.05$; **, $p < 0.01$; ***, $p < 0.001$

				Firing Frequency	
Genotype	Age	Mice (*N*)	Cells (*n*)	Steady-state	Instantaneous
				Hz	Hz
H/H	P16-21	3	11	226 ± 14**	246 ± 12***
H/+	P16-21	5	22	283 ± 10	314 ± 10
	6-mo	3	29	199 ± 22***	245 ± 24***
+/+	P16-21	3	13	294 ± 14	327 ± 15
	6-mo	3	25	318 ± 12	401 ± 13
p values (via via One-way ANOVA or unpaired Student's t-test, vs. age-matched +/+ mice)					
P16-21	H/H vs. +/+			0.0018	0.0004
P16-21	H/+ vs. +/+			0.7449	0.680
6-mo	H/+ vs. +/+			<0.0001	<0.0001

Table S7. Firing frequency of neocortex PV+ GABAergic interneurons by genotype and age.
Related to Figure 5.

*, $p < 0.05$; **, $p < 0.01$; ***, $p < 0.001$

				Intrinsic Membrane Properties				
Brain Region	Genotype	Mice (*N*)	Cells (*n*)	V_m	R_m	Tau	Sag	Rheobase
				mV	MOhms	ms	%	pA
CA3	H/+	5	17	-55.1 ± 1.2	84.3 ± 11.0	9.5 ± 0.9	33 ± 5**	186 ± 18
	+/+	3	8	-54.8 ± 1.5	159 ± 43	10.6 ± 1.1	11 ± 2	160 ± 24
RTN	H/+	4	34	-59.6 ± 2.4	230 ± 15	14.4 ± 0.9	7 ± 1	59 ± 8
	+/+	3	13	-57.9 ± 2.6	428 ± 70	14.9 ± 1.3	5 ± 1	44 ± 13
IC	H/+	2	25	-61.0 ± 1.1	84.2 ± 15.8	5.1 ± 0.6	169 ± 18	161 ± 20
	+/+	2	24	-61.8 ± 1.1	62.9 ± 13.6	4.0 ± 0.3	178 ± 23	203 ± 21
p values (via via One-way ANOVA or unpaired Student's t-test, vs. age-matched +/+ mice)								
CA3				0.894	0.169	0.500	0.002	0.452
RTN				0.158	0.009	0.374	0.648	0.969
IC				0.595	0.313	0.111	0.766	0.153

Table S8. Intrinsic membrane properties of Kv3.1-expressing PV+ neurons in H/+ vs. wild-type mice. Related to Figure 5.

*, $p < 0.05$; **, $p < 0.01$; ***, $p < 0.001$. CA3, hippocampal CA3; IC, inferior colliculus; RTN, thalamic reticular nucleus. All recordings performed at P16-21.

				Action Potential Properties									
Group	Age	Mice (N)	Cells (n)	Inflection Rate	Max Rise Slope	AP Thres-hold	AP Amp-litude	AP Peak	AP Rise Time	AP Halfwidth	AHP Amp-litude	AHP Time	ISI CoV
				mV/ms	mV/ms	mV	mV	mV	ms	ms	mV	ms	
CA3	H/+	5	17	12.1 ± 2.6	664 ± 60**	-44.4 ± 1.5	86.8 ± 3.3*	42.3 ± 2.6*	0.50 ± 0.03	0.34 ± 0.02	-18.4 ± 1.1	1.00 ± 0.11	0.18 ± 0.03
	+/+	3	8	26.4 ± 6.7	457 ± 25	-44.2 ± 1.9	75.7 ± 2.9	31.5 ± 3.0	0.44 ± 0.03	0.32 ± 0.01	-18.8 ± 1.7	0.84 ± 0.03	0.21 ± 0.05
RTN	H/+	4	34	15.2 ± 2.1	491 ± 32	-42.8 ± 0.5*	80.8 ± 1.9	38.1 ± 1.8	0.62 ± 0.05	0.39 ± 0.03	-15.5 ± 0.8	1.05 ± 0.08	0.26 ± 0.02***
	+/+	3	13	25.5 ± 5.7	452 ± 29	-40.3 ± 2.0	79.8 ± 3.1	39.5 ± 2.6	0.54 ± 0.06	0.38 ± 0.02	-16.5 ± 1.6	1.30 ± 0.32	0.17 ± 0.02
IC	H/+	2	25	5.5 ± 0.7	222 ± 9	-41.2 ± 0.9	53.5 ± 1.5	12.3 ± 1.9	0.67 ± 0.02	0.38 ± 0.02	-19.4 ± 0.8	1.02 ± 0.14	0.24 ± 0.03
	+/+	2	24	4.0 ± 0.4	238 ± 6	-42.9 ± 1.0	55.6 ± 1.2	12.7 ± 1.2	0.73 ± 0.04	0.36 ± 0.02	-16.9 ± 1.0	0.74 ± 0.05	0.33 ± 0.03
p values (via via One-way ANOVA or unpaired Student's t-test, vs. age-matched +/+ mice)													
CA3				0.110	0.008	0.922	0.030	0.026	0.292	0.369	0.883	0.197	0.645
RTN				0.143	0.762	0.040	0.890	0.286	0.570	0.777	0.065	0.415	0.0002
IC				0.070	0.139	0.239	0.279	0.839	0.244	0.458	0.059	0.082	0.0637

Table S9. Action potential properties of Kv3.1-expressing PV+ neurons in H/+ vs. wild-type mice. Related to Figure 4-5.

*, $p < 0.05$; **, $p < 0.01$; ***, $p < 0.001$. CA3, hippocampal CA3; IC, inferior colliculus; RTN, thalamic reticular nucleus. All recordings performed at P16-21.

				Firing Frequency	
Group	Age	Mice (*N*)	Cells (*n*)	Steady-state	Instantaneous
				Hz	Hz
CA3	H/+	5	17	219 ± 13	286 ± 18
	+/+	3	8	253 ± 16	319 ± 13
RTN	H/+	4	34	178 ± 10	287 ± 10
	+/+	3	13	209 ± 13	300 ± 15
IC	H/+	2	25	259 ± 20	385 ± 17*
	+/+	2	24	288 ± 26	442 ± 12
CA3				0.163	0.183
RTN				0.175	0.889
IC				0.380	0.010

Table S10. Firing frequency of Kv3.1-expressing PV+ neurons in H/+ vs. wild-type mice. Related to Figure 4-5.

*, $p < 0.05$; **, $p < 0.01$; ***, $p < 0.001$. CA3, hippocampal CA3; IC, inferior colliculus; RTN, thalamic reticular nucleus. All recordings performed at P16-21.